Time Domain Integral Equation Based Analysis for Thin Scatterers Using Impedance Boundary Conditions

Qin Chen*, Mingyu Lu, Meng Lu, and Eric Michielssen
Center for Computational Electromagnetics
Department of Electrical and Computer Engineering
University of Illinois at Urbana-Champaign, Urbana, IL 61801
qinchen@uiuc.edu

1 Introduction

Impedance boundary conditions (IBCs) relate electric and magnetic fields tangential to smooth material surfaces of highly conductive objects. The usage of IBC models in electromagnetic field simulators eliminates the need to model a scatterer's internal fields, thereby leaving only exterior scattering problems to be solved. In this paper, the time domain integral equation (TDIE) solver for analyzing scattering from nontransparant IBC objects reported in [1] is extended to analyze scattering from electrically thin, and potentially penetrable IBC surfaces [2]. Two coupled TDIEs that are very similar to those in [1] are established and solved by marching-on-in-time (MOT). The proposed scheme is verified by means of several numerical examples.

2 TDIE solvers for thin scatterers with IBC

Consider a thin, surface-like scatterer S of thickness d, composed of a homogeneous material with frequency independent permeability μ, permittivity ε, and conductivity σ, residing in free space with permittivity ε_0 and permeability μ_0, and excited by a bandlimited incident field $\left(\mathbf{E}^{inc}(\mathbf{r},t),\mathbf{H}^{inc}(\mathbf{r},t)\right)$ with spectral support confined to $[\omega_{min},\omega_{max}]$ and virtually zero for any point on the scatterer when $t<0$. Upon excitation by the incident field, S produces the scattered field $\left(\mathbf{E}^{sca}(\mathbf{r},t),\mathbf{H}^{sca}(\mathbf{r},t)\right)$. The total field $\left(\mathbf{E}^{tot}(\mathbf{r},t),\mathbf{H}^{tot}(\mathbf{r},t)\right)$ comprises the incident and scattered fields. In what follows, it is assumed that $d \ll \lambda_{\min} = 2\pi c/\omega_{max}$, where $c = 1/\sqrt{\varepsilon_0\mu_0}$. If for all angular frequencies $\omega \in [\omega_{min},\omega_{max}]$, $|\varepsilon'\mu| \gg |\varepsilon_0\mu_0|$ (with $\varepsilon' = \varepsilon + \sigma/(j\omega)$) and S's minimum radius of curvature is much larger than the skin depth $\delta = \sqrt{2/\omega\mu\sigma}$, then the tangential components of the total fields on the scatterer's opposite interfaces approximately satisfy the following boundary conditions:

$$\begin{bmatrix} -\hat{\mathbf{n}}(\mathbf{r}^+) \times \hat{\mathbf{n}}(\mathbf{r}^+) \times \mathbf{E}^{tot}(\mathbf{r}^+,t) \\ -\hat{\mathbf{n}}(\mathbf{r}^-) \times \hat{\mathbf{n}}(\mathbf{r}^-) \times \mathbf{E}^{tot}(\mathbf{r}^-,t) \end{bmatrix} = \begin{bmatrix} A(t) & B(t) \\ B(t) & A(t) \end{bmatrix} * \begin{bmatrix} \hat{\mathbf{n}}(\mathbf{r}^+) \times \mathbf{H}^{tot}(\mathbf{r}^+,t) \\ \hat{\mathbf{n}}(\mathbf{r}^-) \times \mathbf{H}^{tot}(\mathbf{r}^-,t) \end{bmatrix}, \quad \begin{array}{l} \mathbf{r}^+ \in S^+ \\ \mathbf{r}^- \in S^- \end{array}. \quad (1)$$

Here, S^+ and S^- denote S's "upper" and "lower" interfaces to free space (Fig. 1(a)), $\hat{\mathbf{n}}(\cdot)$ is the outward pointing normal unit vector, " $*$ " denotes temporal convolution, $A(t)$

and $B(t)$ are the inverse Fourier transforms of $\tilde{A}(\omega) = -j\eta\cot(\beta d)$ and $\tilde{B}(\omega) = -j\eta\csc(\beta d)$, respectively; $j = \sqrt{-1}$, $\eta = \sqrt{\mu/\varepsilon'}$, and $\beta = \omega\sqrt{\mu\varepsilon'}$. The boundary conditions in (1) are the time domain counterparts of the frequency domain conditions presented in [2]. When d is very large compared to the skin depth, the boundary conditions in (1) reduce to the regular IBCs in [1]; on the other hand, when d is so small that $\beta d \to 0$, they become equivalent to the regular conducting sheet model. Integral equations that permit reconstruction of $\left(\mathbf{E}^{sca}(\mathbf{r},t), \mathbf{H}^{sca}(\mathbf{r},t)\right)$ are established by invoking the equivalence principle (Fig. 1(b)), viz. by describing $\left(\mathbf{E}^{sca}(\mathbf{r},t), \mathbf{H}^{sca}(\mathbf{r},t)\right)$ in terms of equivalent electric and magnetic currents on S^+ and S^-. However, since $d \ll \lambda_{\min}$, the scattered field $\left(\mathbf{E}^{sca}(\mathbf{r},t), \mathbf{H}^{sca}(\mathbf{r},t)\right)$ can be described by the superposition of these equivalent currents on both interfaces, viz. as produced by electric and magnetic current $\mathbf{J}(\mathbf{r},t) = \hat{n}(\mathbf{r}^+)\times\mathbf{H}^{tot}(\mathbf{r}^+,t) + \hat{n}(\mathbf{r}^-)\times\mathbf{H}^{tot}(\mathbf{r}^-,t)$ and $\mathbf{K}(\mathbf{r},t) = \mathbf{E}^{tot}(\mathbf{r}^+,t)\times\hat{n}(\mathbf{r}^+) + \mathbf{E}^{tot}(\mathbf{r}^-,t)\times\hat{n}(\mathbf{r}^-)$ with $\mathbf{r} = \left(\mathbf{r}^+ + \mathbf{r}^-\right)/2$ on S. Using (1) and $\hat{n}(\mathbf{r}^+) = -\hat{n}(\mathbf{r}^-)$, the following coupled TDIEs in terms of $\mathbf{J}(\mathbf{r},t)$ and $\mathbf{K}(\mathbf{r},t)$ are arrived at:

$$-\frac{\partial}{\partial t}\left\{R_s(t) * \mathbf{J}(\mathbf{r},t)\right\} = \hat{n}(\mathbf{r})\times\hat{n}(\mathbf{r})\times\left\{\mathcal{L}\{\mathbf{J}\}(\mathbf{r},t) - \mathcal{K}\{\mathbf{K}\}(\mathbf{r},t) + \frac{\partial}{\partial t}\mathbf{E}^{inc}(\mathbf{r},t)\right\}$$
$$-\frac{\partial}{\partial t}\left\{G_s(t) * \mathbf{K}(\mathbf{r},t)\right\} = \hat{n}(\mathbf{r})\times\hat{n}(\mathbf{r})\times\left\{\frac{\varepsilon_0}{\mu_0}\mathcal{L}\{\mathbf{K}\}(\mathbf{r},t) + \mathcal{K}\{\mathbf{J}\}(\mathbf{r},t) + \frac{\partial}{\partial t}\mathbf{H}^{inc}(\mathbf{r},t)\right\} \quad (2)$$

Here the operators $\mathcal{L}$ and $\mathcal{K}$ are

$$\mathcal{L}\{\mathbf{X}(\mathbf{r},t)\}(\mathbf{r},t) = -\mu_0\iint_S\left(\frac{\partial^2}{\partial t^2}\overline{\mathbf{I}} - c^2\nabla\nabla\right)\cdot\mathbf{X}(\mathbf{r}',t) * G(|\mathbf{r}-\mathbf{r}'|,t)d\mathbf{r}'$$
$$\mathcal{K}\{\mathbf{X}(\mathbf{r},t)\}(\mathbf{r},t) = \frac{\partial}{\partial t}\nabla\times\!\!\iint_S\mathbf{X}(\mathbf{r}',t) * G(|\mathbf{r}-\mathbf{r}'|,t)d\mathbf{r}' \quad (3)$$

where $\iint$ stands for principle value integration, $\overline{\mathbf{I}} = \hat{x}\hat{x} + \hat{y}\hat{y} + \hat{z}\hat{z}$, and the scalar Green function is $G(r,t) = \delta(t - r/c)/4\pi r$. The surface impedance $R_s(t)$ and admittance $G_s(t)$ are the inverse Fourier transforms of $\tilde{R}_s(\omega) = \left[\tilde{A}(\omega) + \tilde{B}(\omega)\right]/2$ and $\tilde{G}_s(\omega) = 1/\left[2\tilde{A}(\omega) - 2\tilde{B}(\omega)\right]$, respectively. The TDIEs in (2) are very similar to those in [1]. They can be solved using the same MOT scheme as detailed in [1]. Also as in [1], the evaluation of the two temporal convolutions involving $R_s(t)$ and $G_s(t)$ can be accelerated by a recursive convolution technique. However, additional care is needed in that $R_s(t)$ and $G_s(t)$ do not have closed form expressions and hence have to be obtained by means of numerical inverse Fourier transformation.

3 Numerical examples

In this section, two numerical examples are presented to validate the proposed scheme. In the first example, the scatterer is a penetrable spherical shell with outer radius 1.4 m. The shell is centered at the spatial origin and has material parameters $\varepsilon = \varepsilon_0$ and $\mu = \mu_0$, various conductivities and thicknesses are considered. The incident field is parameterized as

$$\mathbf{E}^{inc}(\mathbf{r},t) = \hat{\mathbf{p}}\cos\left[2\pi f_0(t - \mathbf{r}\cdot\hat{\mathbf{k}}/c - t_p)\right]\exp\left[-(t - \mathbf{r}\cdot\hat{\mathbf{k}}/c - t_p)^2/2\upsilon^2\right], \quad (4)$$

where $\hat{\mathbf{p}} = \hat{\mathbf{x}}$, $\hat{\mathbf{k}} = \hat{\mathbf{z}}$, $f_0 = 100$ MHz, $\upsilon = 0.95\times10^{-8}$ s and $t_p = 5.72\times10^{-8}$ s. There are 10592 spatial and 1000 temporal discrete unknowns respectively, and the time step size is 3.33×10^{-10} s. The MOT results are Fourier transformed to the frequency domain and compared to the analytical results. In Fig. 2, the radar cross section (RCS) is plotted at three frequencies: 80 MHz, 100 MHz, and 120 MHz. Figures 2(a) and 2(b) show the RCS data in the x-y and y-z planes, respectively, when $\sigma = 10$ S/m and $d = 0.005\text{m} = 0.31\delta_0$ with δ_0 as the skin depth at frequency f_0. Figures 2(c) and 2(d) show the same data but for $\sigma = 10^5$ S/m and $d = 0.00005\text{m} = 0.31\delta_0$. Figures 2(a) to 2(d) reveal that the TDIE solver generates correct results over a wide range of conductivity values. Next, scattering from a two-plate scatterer shown in Fig. 3(a) is analyzed. The incident field is the same as that in the first example except that $\hat{\mathbf{p}} = \hat{\mathbf{y}}$ and $\hat{\mathbf{k}} = \sin(\pi/6)\hat{\mathbf{x}} + \cos(\pi/6)\hat{\mathbf{z}}$. The scatterer has material parameters $\varepsilon = \varepsilon_0$, $\mu = \mu_0$, $\sigma = 10$ S/m and $d = 0.005\text{m} = 0.31\delta_0$. There are 5520 spatial unknowns on each plate, and the TDIE solver is run for 1000 time steps with time step size 3.33×10^{-10} s. For comparison purposes, this problem is also analyzed using a finite difference time domain (FDTD) simulator [3] that incorporates the IBCs in (1). Figures 3(b) and (c) show the equivalent current J_y and K_x at one point on the lower plate specified by $(1.5333, 1.5333,0)$ m. There is an excellent agreement between the MOT and FDTD waveforms. The time domain results from the MOT and FDTD are both Fourier transformed to the frequency domain, and the RCS in the y-z plane are compared in Fig. 3(d) at three frequencies: 80 MHz, 100 MHz, and 120 MHz. The RCS results from the MOT and FDTD simulations match each other very well.

References

[1]   Q. Chen, M. Lu, and E. Michielssen, "Integral equation based analysis of transient scattering from surfaces with impedance boundary condition," *Microwave and Optical Technology Letters*, vol. 42, pp. 213-220, 2004.

[2]   E. Bleszynski, M. Bleszynski, and T. Jaroszewicz, "Surface-integral equations for electromagnetic scattering from impenetrable and penetrable sheets," *IEEE Antennas and Propagation Magazine*, vol. 35, pp. 14-25, 1993.

[3]   J. G. Maloney and G. S. Smith, "The use of surface impedance concepts in the finite-difference time-domain method," *IEEE Transactions on Antennas and Propagation*, vol. 40, pp. 38-48, 1992.

(a) The original problem   (b) An equivalent problem to that in (a)
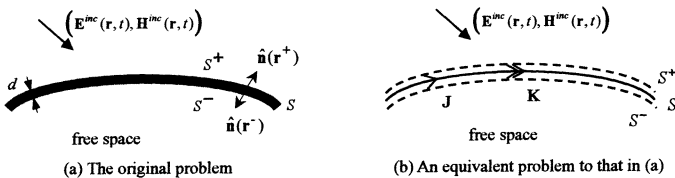
Figure 1: Illustration of the scattering problem of concern

(a) RCS in the x-y plane ($\sigma = 10$ S/m)

(b) RCS in the y-z plane ($\sigma = 10$ S/m)

(c) RCS in the x-y plane ($\sigma = 10^5$ S/m)

(d) RCS in the y-z plane ($\sigma = 10^5$ S/m)
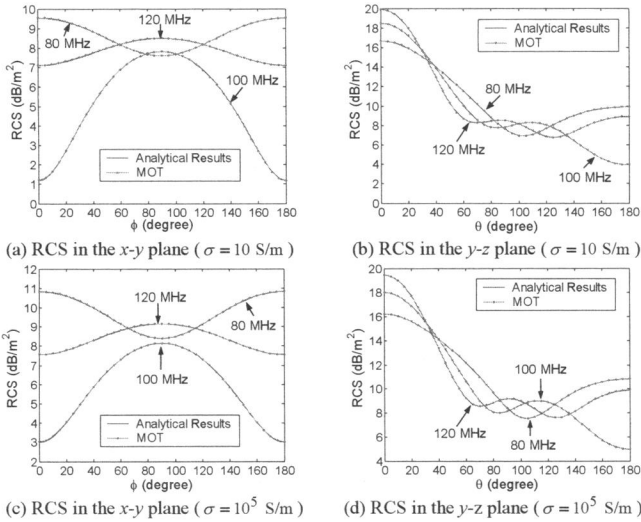
Figure 2: Numerical results for the scattering from spherical shells ($d = 0.31\delta_0$)

(a) Illustration of the two-plate scatterer

(b) J_y at the center of the lower plate

(c) K_x at the center of the lower plate

(d) RCS in the y-z plane
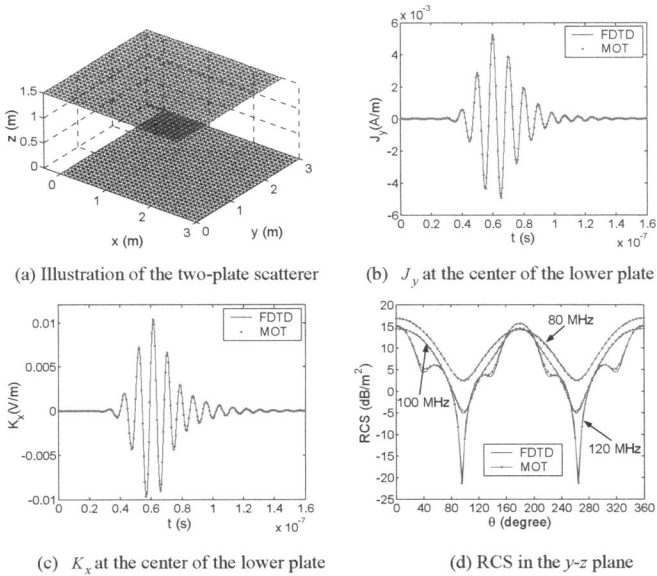
Figure 3: Numerical results for the scattering from a two-plate scatterer